Nucleation and Growth of $Cu_{33}Al_{17}$ in Al-Modified Lead-Free Sn-Ag-Cu and Sn-Cu Solder Alloys

Kathlene N. Lindley [1,2], Iver E. Anderson [2,3], Carol A. Handwerker [1]

[1] Materials Engineering Department, Purdue University, West Lafayette, IN, USA, 47907
[2] Division of Material Science and Engineering, Ames Laboratory (USDOE), Ames, IA, USA, 50011
[3] Material Science and Engineering Department, Iowa State University, Ames, IA, USA, 50011

Introduction:

Many lead-free solder alloys based on the Sn-Ag-Cu (SAC) ternary eutectic (T_{eut} = 217°C) system have been proposed throughout the years with a wide array of applications, especially concerning microelectronic ball grid array (BGA) systems. This work aims to decipher the nucleation behavior and growth of $Cu_{33}Al_{17}$ intermetallic, a faceted particle phase, based on small variations of both Cu wt.% (0.34-3.0%) and Al wt.% (0.0-0.4%) within as-cast microalloyed SAC+Al and Sn-Cu (SC) + Al solders wires and within SAC+Al BGA joints.

Ultimate Goal: Control the fundamental solder nucleation processes within microelectronic BGAs through specified additions of Al to solders systems.

- **Benefits of Al Additions in Solder Alloys:**
  - Al additions provide *a **notable reduction in undercooling*** to SAC solders, all while maintaining solder melt temperature. [1]
  - Al additions ***increase suppression of the Ag_3Sn blade phase*** within SAC solders. This phase has detrimental embrittlement effects to the overall performance of SAC solder joints. [1]
  - Al additions, in SAC & SC solders, promote the ***formation of a beneficial $Cu_{33}Al_{17}$ faceted particle phase***. This phase provides benefits through:
    - ***Extraordinary hardness***: found to range from 30-50 GPa, depending on the base hardness of the surrounding matrix. This could potentially produce beneficial particle hardening effects within the solders. [1]
    - ***Low density***: $Cu_{33}Al_{17}$ particles are buoyant within molten Sn. This buoyancy could prove to be useful within BGAs, where most of the fatigue occurs at the top interface between the solder and the ceramic substrate. [1]
    - ***Initial nucleation sites***: Evidence shows that $Cu_{33}Al_{17}$ is likely the first phase to form within these solder systems, and that it persists throughout the solder reflow cycles (due to its high melt/formation temperature). It is hypothesized that this incipient particle formation allows $Cu_{33}Al_{17}$ to act as the ***nucleation agent*** for lower melting intermetallics, such as Cu_6Sn_5, and in turn, for the nucleation of the surrounding Sn matrix. This would allow for ***Sn grain refinement*** within solder BGAs, reducing fatigue, and suppressing crack propagation during thermal cycling. [2]

Experimental Procedure:

- The solder wire samples were produced by the Materials Preparation Center at Ames Laboratory via closed atmosphere drop casting. Full compositions shown in Table I, below. SAC305 & SAC+Al BGAs were provided by Rockwell Collins.
- The solder wire ingots were held at one of two superheat temperatures, 800°C or 1200°C, for 60mins before being solidified via a water quench. The solder ingots were then drawn into 1.7 mm diameter wire.
- The wire alloys were analyzed via SEM, EDS, and DSC, using a ramp up to 1200°C to analyze the wire alloy's ultimate liquidus range. The BGA joints were visually examined via SEM and grain size/orientation was mapped via EBSD.

Table I: Composition, superheat temperature, and particle data on the SAC+Al and SC+Al wire alloys. Compositions and particle data on the SAC305 and SAC+Al solder BGAs also shown.

Sample Number	Sn wt.%	Ag wt.%	Cu wt.%	Al wt.%	Superheat Temperature (°C)	Cu/Al At. %
Sample Series 1: SAC+Al at 1200 °C						
1	95.55	3.50	0.95	0.00	1200	--
2	95.55	3.50	0.90	0.05	1200	1.58
3	95.55	3.50	0.85	0.10	1200	1.78
4	95.55	3.50	0.80	0.15	1200	1.93
5	95.55	3.50	0.75	0.20	1200	Two Phase: 1.32 (Outer), 2.34 (Inner)
6	95.55	3.50	0.70	0.25	1200	1.72
Sample Series 2: SAC+Al at 800 °C						
7	95.55	3.50	0.75	0.20	800	1.58
8	95.55	3.50	0.70	0.25	800	1.68
Sample Series 3: SC+Al at 1200 °C						
9	98.55	0.00	1.25	0.20	1200	1.94
10	96.60	0.00	3.00	0.40	1200	1.97
Sample Series 4: Solder BGA Samples						
SAC 305 BGA	96.50	3.00	0.50	0.00	--	--
SAC+Al BGA	96.30	3.27	0.34	0.02	--	1.70

Results:

- Table I and Fig. 1 & 2 show the particle measurements for the as-cast, solder wire samples. All Al-modified samples produced $Cu_{33}Al_{17}$ particles; verified by the EDS atomic ratio results which approximately match 33:17 (33:17 = 1.94).
- The graph in Fig. 2, along with the visual examples in Fig. 3, provide evidence for the inverse relationship between initial superheat temperature and maximum particle size formation. When referencing the diagram in Fig. 4 and the DSC data shown in Fig. 5, this makes sense, given that time spent at 800°C is below the ultimate alloy liquidus, possibly allowing for convergence and growth of the $Cu_{33}Al_{17}$ particles.

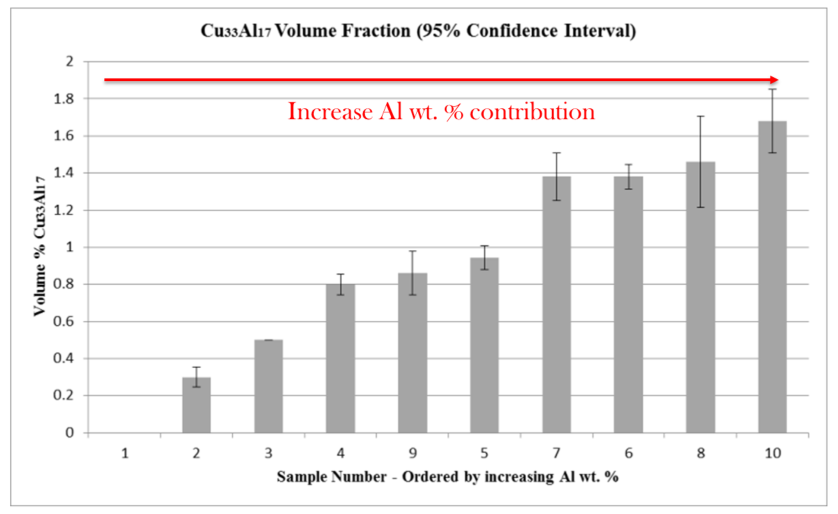

Figure 1: $Cu_{33}Al_{17}$ volume fraction in wire alloys.

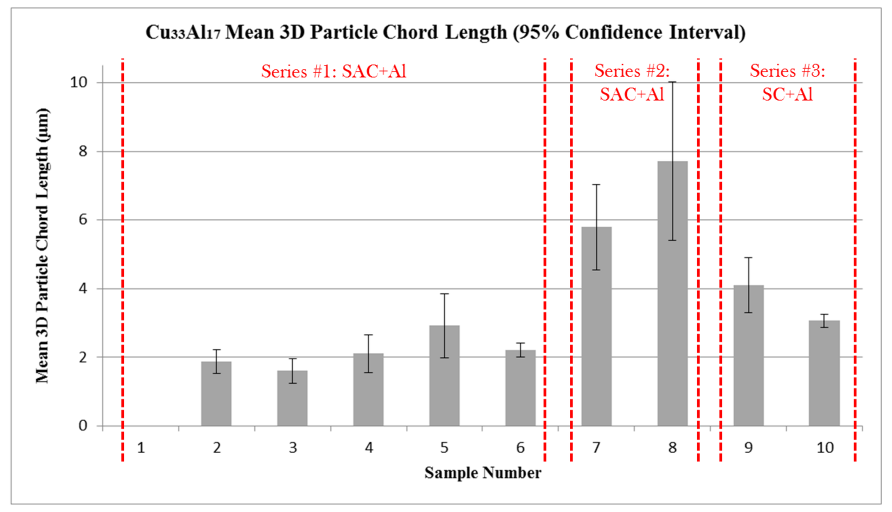

Figure 2: $Cu_{33}Al_{17}$ mean chord length in wire alloys

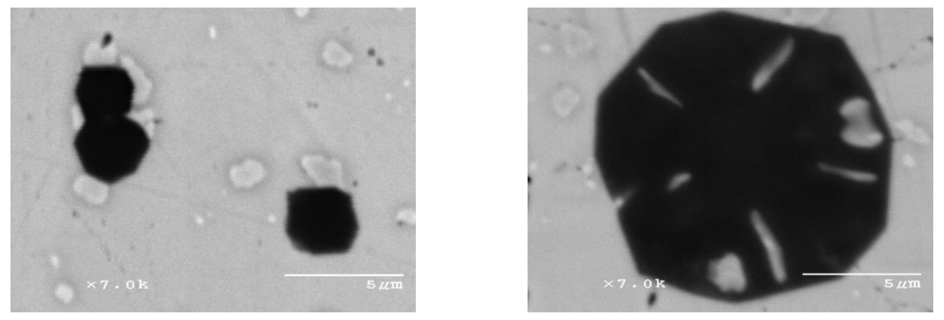

Figure 3: SEM images of $Cu_{33}Al_{17}$ particles within 1200°C Samples 6 (left) & 800°C Sample 8 (right), both taken at 7000x.

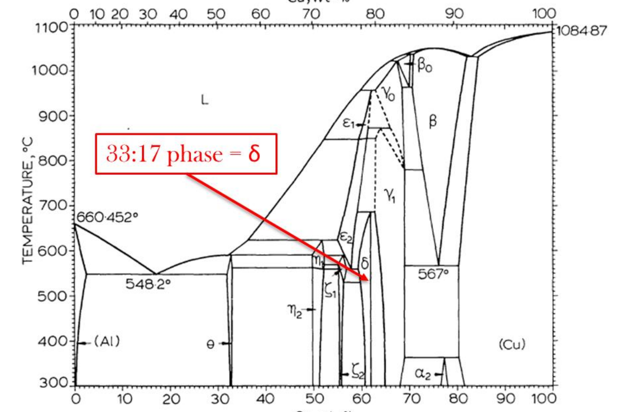

Figure 4: Al-Cu phase diagram. [3]

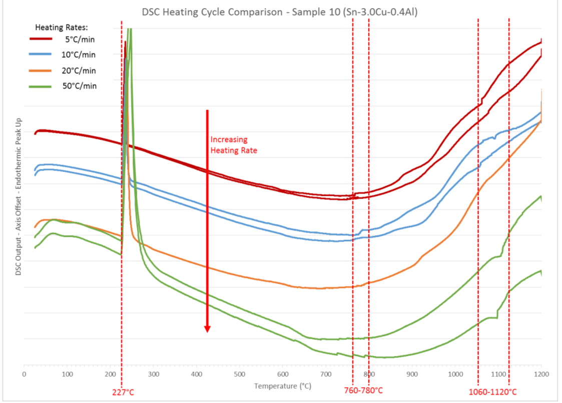

Figure 5: Overlay view of DSC heating cycle on Sample 10.

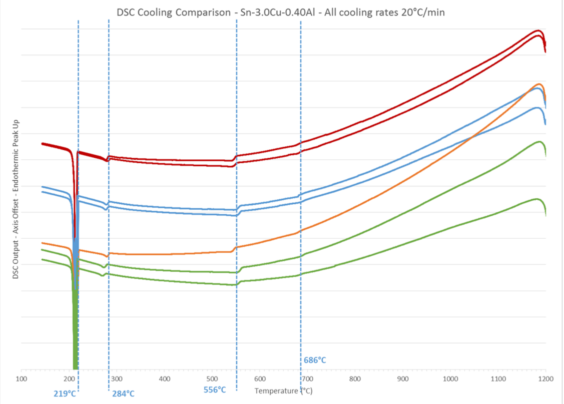

Figure 6: Overlay view of DSC cooling cycle of Sample 10.

- DSC results shown in Figs. 5 & 6, conducted on Sample 10, due to the sample's high $Cu_{33}Al_{17}$ vol. %, show the heating and cooling events of the solder alloy. The ultimate alloy liquidus range was identified between 1060-1120°C. The cooling curves agree well for the solidification range identified for the $Cu_{33}Al_{17}$ phase within the phase diagram in Fig. 4.

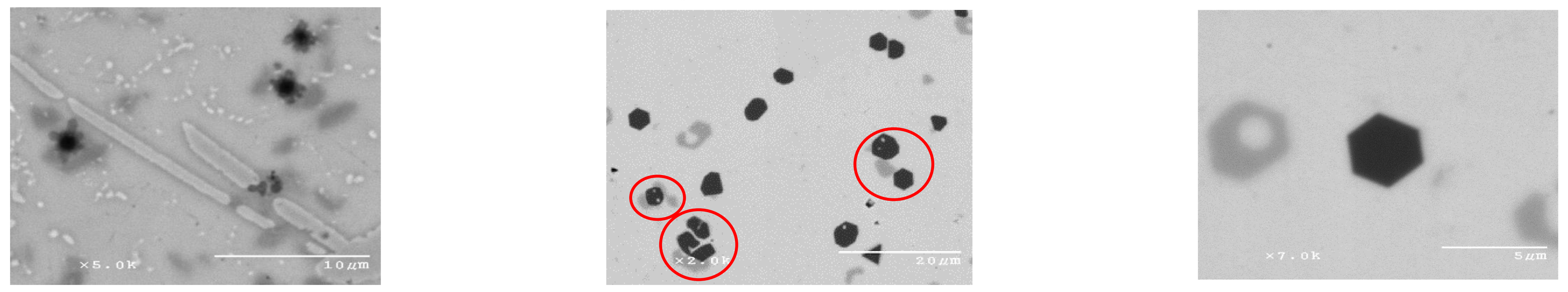

Figure 7: SAC+Al BGA (left) showing Cu_6Sn_5 "flower petal" nucleation on surface of $Cu_{33}Al_{17}$ particles, Sample 10 (2000x, middle & 7000x, right) highlighting the "shadowing" of $Cu_{33}Al_{17}$ by Cu_6Sn_5.

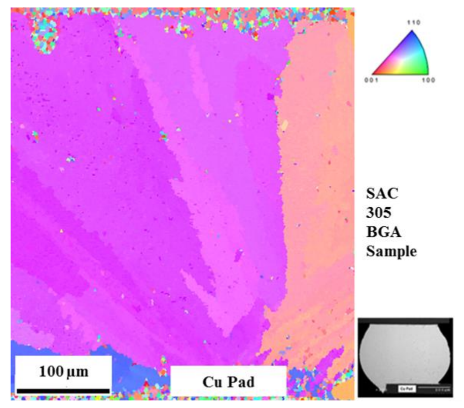

Figure 8:

SAC305 EBSD grain map showing ~2 Sn grains (left).

SAC+Al EBSD grain map showing ~4-5 Sn grains (right).

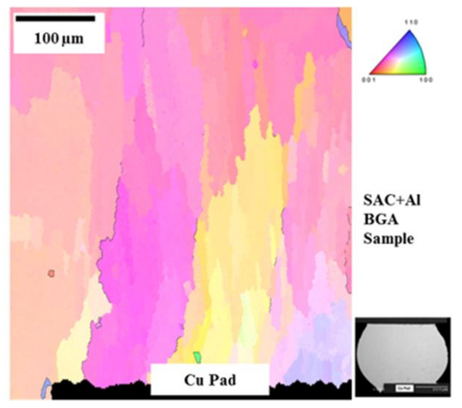

- Visual examination coupled with the DSC results support the hypothesis that $Cu_{33}Al_{17}$ forms first within the solders and then acts as a nucleation agent for the Cu_6Sn_5 intermetallic phase, which then nucleates the surrounding Sn matrix. This is seen through the Cu_6Sn_5 "flower petal" formation surrounding the $Cu_{33}Al_{17}$ particles in the BGA in Fig. 7, and also through the "shadowing" of $Cu_{33}Al_{17}$ by Cu_6Sn_5 in Sample 10 in Fig. 7. EBSD results (see Fig. 8) also show slight Sn grain refinement within the SAC+Al BGA, even at an Al wt.% = 0.015, as compared to baseline SAC305 BGA sample.

Conclusions & Future Work:

- **Summarized Results:**
  - $Cu_{33}Al_{17}$ particle formation was observed within all of the tested as-cast, Al-modified solder wire alloys and within the SAC+Al BGA solder sample.
  - Possible particle coarsening/convergence was seen at the 800°C superheat temperature, resulting in higher maximum $Cu_{33}Al_{17}$ particles sizes.
  - DSC heating cycle data showed a high temperature, final liquidus of the ternary, SC+Al , alloy within the range of 1060-1120°C, and the cooling cycle curves show possible solidification events for the $Cu_{33}Al_{17}$, Cu_6Sn_5, and the final solder Sn matrix. The average undercooling was measured to be ~8°C.
  - Visual examinations, DSC, and EBSD mapping provided evidence to support the hypothesis that $Cu_{33}Al_{17}$ particles are the first phase to form during solidification of the solder alloys. It is further hypothesized, with the support of the compiled results, that these particles then act as a nucleation agent for Cu_6Sn_5 intermetallic, followed by the Sn matrix, which has a refined grain structure due to the Al additions in the BGA joint.
- **Future Work:**
  - Perform solidification studies between various solder alloy and bulk $Cu_{33}Al_{17}$ samples in order to decipher the orientation relationship between the solder constituents and the surface of $Cu_{33}Al_{17}$.
  - Perform further EBSD analysis on SAC vs. SAC+Al BGA samples with varying Al contents to more thoroughly determine the correlation between the Al addition, $Cu_{33}Al_{17}$ particle formation, and the overall Sn grain refinement seen within the joints.

References:
[1] Boesenberg, A. J., I. E. Anderson, and J. L. Harringa. "Development of Sn-Ag-Cu-X Solders for Electronic Assembly by Micro-Alloying with Al." Journal of Electronic Materials Vol. 41, No. 7, Pp. 1868-1881. (2012).
[2] Lindley, K.L., I.E. Anderson. "The Nucleation and Growth of $Cu_{33}Al_{17}$ in Al Modified Sn-Ag-Cu and Sn-Cu Pb-Free Solder Alloys." Journal of Electronic Materials. (Accepted, under revisions: January 2014).
[3] Murray J. L., Al-Cu Phase Diagram, 1990, ASM Alloy Phase Diagrams Center, P. Villars, editor-in-chief; H. Okamoto and K. Cenzual, section editors; http://www1.asminternational.org/AsmEnterprise/APD, ASM International, Materials Park, OH, 2006-2013.

Acknowledgements:
Work at the Ames Laboratory was supported by the U.S. DOE Science Undergraduate Laboratory Internship (SULI) Program under its contract with Iowa State University, Contract No. DE-AC02-07CH11358. The research group is grateful to the DOE for the assistantship and opportunity to participate in the SULI program. The group would like to also thank Fran Laabs (laabs@ameslab.gov), of Ames Laboratory, for gathering the EBSD data.